

•Research article•

Design, synthesis, and biological evaluation of ligustrazine/resveratrol hybrids as potential anti-ischemic stroke agents

ZHANG Yin-Qiu^Δ, WU Jian-Bing^Δ, YIN Wei, ZHANG Yi-Hua^{*}, HUANG Zhang-Jian^{*}

State Key Laboratory of Natural Medicines, Jiangsu Key Laboratory of Drug Discovery for Metabolic Diseases, Center of Drug Discovery, China Pharmaceutical University, Nanjing 210009, China

Available online 20 Aug., 2020

[ABSTRACT] To search for potent anti-ischemic stroke agents, a series of tetramethylpyrazine (TMP)/resveratrol (RES) hybrids **6a–t** were designed and synthesized. These hybrids inhibited adenosine diphosphate (ADP)- or arachidonic acid (AA)-induced platelet aggregation, among them, **6d**, **6g–i**, **6o** and **6q** were more active than TMP. The most active compound **6h** exhibited more potent anti-platelet aggregation activity than TMP, RES, as well as positive control ticlopidine (Ticlid) and aspirin (ASP). Furthermore, **6h** exerted strong antioxidative activity in a dose-dependent manner in rat pheochromocytoma PC12 cells which were treated with hydrogen peroxide (H₂O₂) or hydroxyl radical (·OH). Importantly, **6h** significantly protected primary neuronal cells suffered from oxygen-glucose deprivation/reoxygenation (OGD/R) injury, comparable to an anti-ischemic drug edaravone (Eda). Together, our findings suggest that **6h** may be a promising candidate warranting further investigation for the intervention of ischemic stroke.

[KEY WORDS] Ligustrazine; Resveratrol; Hybrids; Anti-platelet aggregation; Antioxidant; Ischemic stroke

[CLC Number] R914.5, R965 **[Document code]** A **[Article ID]** 2095-6975(2020)08-0633-08

Ischemic stroke with high morbidity, mortality, disability and recurrence rates remains a leading cause of death globally [1–4]. Due to its complex pathogenesis, including genetic high risk, thrombosis, and chronic inflammation, *etc.* [5], it is difficult at present to effectively treat this fatal disease. Over the past ten years, great efforts have been made by researchers to combat ischemic stroke, and a large number of anti-platelet aggregation, anticoagulant, neuroprotective, and thrombolytic drugs are available [6–11]. However, the clinical efficacy of these drugs is still unsatisfactory [12], and new therapeutic drugs with good efficacy and safety for the intervention of ischemic stroke are urgently needed.

[Received on] 24-Feb.-2020

[Research funding] This work was supported by the National Natural Science Foundation of China (Nos. 81822041, 81773573, 21977116, and 81673305), the National Science & Technology Major Project “Key New Drug Creation and Manufacturing Program” (No. 2018ZX09711002-006-013), the Open Project of State Key Laboratory of Natural Medicines (No. SKLNMZZCX201824), and the State Key Laboratory of Pathogenesis, Prevention and Treatment of High Incidence Diseases in Central Asia Fund (No. SKL-HIDCA-2018-1), part of the work was supported by the Postgraduate Research & Practice Innovation Program of Jiangsu Province (No. KYCX18_0795).

[*Corresponding author] E-mails: zyhtgd@163.com (ZHANG Yi-Hua); zhangjianhuang@cpu.edu.cn (HUANG Zhang-Jian)

^ΔThese authors contributed equally to this work.

These authors have no conflict of interest to declare.

2, 3, 5, 6-Tetramethylpyrazine (ligustrazine, TMP), a main active ingredient of the Chinese herbal medicine *Ligusticum wallichii Franchet* (Chuanxiong), is able to promote the proliferation and differentiation of the neuronal precursor cells (NPCs) [13, 14] and enhance NPCs migration towards the ischemic region in rats with middle cerebral artery occlusion (MCAO) model [15]. Tetramethylpyrazine nitron (TBN), a ligustrazine derivative, is a potent free radical scavenger with multifunctional neuroprotective effects in rat and monkey models of ischemic stroke [16–18] and has now advanced to Phase II clinical trial for the treatment of ischemic stroke in China.

Resveratrol (RES), 3, 5, 4'-trihydroxy-trans-stilbene, is a poly-phenol compound found in red wine, grapes, and many plants, such as knotweeds and pine trees. RES has multiple functions such as anti-inflammation, anti-oxidation, inhibition of arachidonate acid metabolism [19], and platelet activity [20]. It has been reported that RES reduced brain infarction by inhibition of inducible nitric oxide synthase (iNOS), and upregulation of endothelial nitric oxide synthase (eNOS) expression in MCAO rats model [21]. Other studies suggested that RES attenuated ischemic brain injury *via* inhibition of myeloperoxidase levels, pyrin domain-containing 3 inflammasome (NLRP-3) formation, cerebral TNF- α production, and apoptosis [22–24]. Furthermore, it was reported that RES activated nuclear erythroid 2-related factor 2- and sirtuin-1-mediated pathways to enhance neuronal survival in response to

cerebral ischemia [25, 26]. These investigations suggest that the use of RES may provide benefits in the treatment of cerebral ischemia.

In order to search for more potent anti-ischemic agents than TMP and/or RES, a series of compounds **6a–t** were designed and synthesized by hybridization of TMP with RES (Table 1). Herein, we report the synthesis and biological evaluation of these hybrids.

Results and Discussion

Chemistry

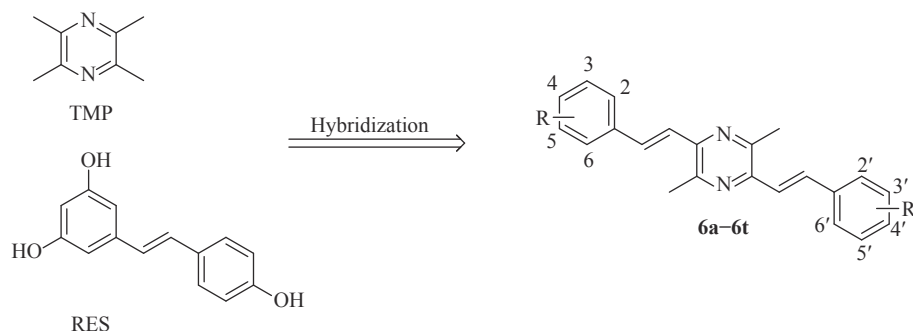
The synthesis of the target compounds **6a–6t** is depicted in Scheme 1. Generally, treatment of TMP with 30% hydrogen peroxide aqueous solution produced pyrazine 1, 4-dioxide **1**, which was heat at reflux in acetic anhydride *via* a Boekelheide rearrangement reaction to furnish diacetate derivative **2**. Subsequently, hydrolysis of **2** in a 20% aqueous

sodium hydroxide solution provided dihydroxy compound **3**, followed by treatment with phosphorus tribromide to give brominated derivative **4**. The phosphate ester **5** was obtained by the reaction of **4** with triethyl phosphite. Finally, treatment of **5** with corresponding substituted benzaldehydes in the presence of sodium hydride *via* the Wittig-Horner reaction afforded **6a–6t**. All the target compounds with a chemical purity of > 95% (determined by HPLC analysis) were used for following biological experiments.

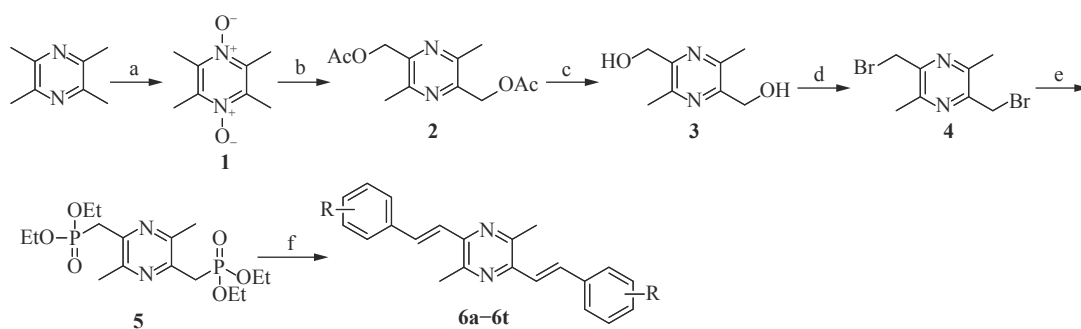
In vitro anti-platelet aggregation

Firstly, we evaluated the *in vitro* inhibitory effects of the target compounds on the adenosine diphosphate (ADP)- and arachidonic acid (AA)-induced platelet aggregation in rabbit platelet-rich plasma (PRP) by Born's turbidimetric method. Ticlopidine hydrochloride (Ticlid) and aspirin (ASP), as inhibitors of adenosine diphosphate (ADP)- and arachidonic acid (AA)-induced platelet aggregation, respectively [27, 28],

Table 1 Chemical structures of compounds **6a–6t**



Compounds	R substituents			
	2, 2'	3, 3'	4, 4'	5, 5'
6a	H	H	H	H
6b	H	OCH ₃	OCH ₃	H
6c	H	OCH ₃	OH	H
6d	H	OCH ₃	OCH ₃	OCH ₃
6e	H	H	OCH ₃	H
6f	H	Br	OCH ₃	H
6g	OCH ₃	H	H	H
6h	H	H	OH	H
6i	OH	H	H	H
6j	H	H	CH ₃	H
6k	H	CH ₃	H	H
6l	CH ₃	H	H	H
6m	Cl	H	H	H
6n	H	H	Cl	H
6o	H	H	Br	H
6p	H	OCH ₃	H	H
6q	H	OH	H	H
6r	OCH ₃	H	OCH ₃	H
6s	H	H	N(CH ₃) ₂	H
6t	H	H	F	H



Scheme 1 Synthetic route of compounds **6a–6t**. Reagents and conditions: (a) 30% H_2O_2 , AcOH, 95 °C, 8 h; (b) Ac_2O , reflux, 2.5 h; (c) 20% NaOH, rt, overnight; (d) CH_2Cl_2 , PBr_3 , 0.5 h; (e) $(\text{C}_2\text{H}_5\text{O})_3\text{P}$, reflux, 1 h; (f) THF, NaH, corresponding aldehydes, 0 °C, 0.5 h

Table 2 The IC_{50} values of compounds **6a–6t** against platelet aggregation *in vitro* induced by ADP or AA (mean \pm SD, $n = 5$)

Compound	$\text{IC}_{50}/(\text{mmol}\cdot\text{L}^{-1})$	
	ADP ($10\ \mu\text{mol}\cdot\text{L}^{-1}$)	AA ($1\ \text{mmol}\cdot\text{L}^{-1}$)
Ticlopid ^a	0.29 \pm 0.11	-
ASP ^b	-	0.15 \pm 0.09
6a	1.21 \pm 0.26	0.78 \pm 0.06
6b	1.18 \pm 0.17	0.80 \pm 0.12
6c	1.28 \pm 0.21	0.99 \pm 0.11
6d	0.83 \pm 0.08	0.61 \pm 0.24
6e	1.30 \pm 0.25	0.99 \pm 0.14
6f	1.17 \pm 0.18	0.72 \pm 0.26
6g	0.96 \pm 0.13	0.57 \pm 0.04
6h	0.12 \pm 0.04	0.07 \pm 0.01
6i	0.31 \pm 0.07	0.19 \pm 0.05
6j	1.99 \pm 0.30	1.18 \pm 0.21
6k	1.91 \pm 0.26	1.74 \pm 0.17
6l	2.55 \pm 0.34	2.26 \pm 0.24
6m	1.81 \pm 0.18	1.47 \pm 0.13
6n	1.08 \pm 0.07	0.77 \pm 0.11
6o	1.06 \pm 0.05	0.67 \pm 0.17
6p	3.90 \pm 0.39	3.34 \pm 0.28
6q	0.92 \pm 0.11	0.75 \pm 0.07
6r	1.51 \pm 0.04	1.40 \pm 0.13
6s	2.15 \pm 0.24	1.90 \pm 0.19
6t	1.36 \pm 0.15	1.94 \pm 0.20

^a Ticlopid is an inhibitor of ADP-induced platelet aggregation; ^b ASP is an inhibitor of AA-induced platelet aggregation

were used as positive controls. As shown in Table 2, all the target compounds inhibited the platelet aggregation induced by ADP ($10\ \mu\text{mol}\cdot\text{L}^{-1}$) or AA ($1\ \text{mmol}\cdot\text{L}^{-1}$) to certain degrees, and **6d**, **6g–i**, **6o** and **6q** were more active than TMP.

Notably, the inhibitory activity of the most potent compound **6h** ($\text{IC}_{50}\ 0.12\ \text{mmol}\cdot\text{L}^{-1}$) on ADP-induced platelet aggregation was 10.6-, 5.2-, and 2.4-fold larger than that of TMP ($\text{IC}_{50}\ 1.27\ \text{mmol}\cdot\text{L}^{-1}$), RES ($\text{IC}_{50}\ 0.62\ \text{mmol}\cdot\text{L}^{-1}$), and Ticlid ($\text{IC}_{50}\ 0.29\ \text{mmol}\cdot\text{L}^{-1}$), respectively. Similarly, inhibition of **6h** on AA-induced platelet aggregation ($\text{IC}_{50}\ 0.07\ \text{mmol}\cdot\text{L}^{-1}$) was 11.3-, 7.4-, and 2.1-fold stronger than that of TMP ($\text{IC}_{50}\ 0.79\ \text{mmol}\cdot\text{L}^{-1}$), RES ($\text{IC}_{50}\ 0.52\ \text{mmol}\cdot\text{L}^{-1}$), and ASP ($\text{IC}_{50}\ 0.15\ \text{mmol}\cdot\text{L}^{-1}$), respectively.

The preliminary analysis of structure-activity relationships (SARs) revealed that among compounds with one substituent on each benzene ring, the hydroxy-bearing ones (**6h**, **6i** and **6q**) have better inhibitory activity than others. The general order of activity for one substituent is hydroxy > halogen > methoxy > dimethyl amino > methyl, which might be due to the steric hindrance. In addition, the hydroxyl substituent at the para-position of the benzene ring was preferable (**6h**), as well as halogen substituent (**6n**). Among the compounds with multiple substituents on the benzene ring, the compound possessing three methoxy groups (**6d**) displayed stronger activity than compounds with one or two methoxy groups, probably attributable to the electron donating effects that increase the electron density on the phenyl group which may be beneficial for inhibitory activity on platelet aggregation.

Given that compound **6h** was composed of TMP and RES moieties, we further evaluated the inhibitory effects of each moiety alone or in combination on platelet aggregation *in vitro*. As shown in Table 3, the inhibitory activity of both TMP or RES alone on ADP- or AA-induced platelet aggregation

Table 3 The IC_{50} values of compounds against platelet aggregation *in vitro* (mean \pm SD, $n = 5$)

Compound	$\text{IC}_{50}/(\text{mmol}\cdot\text{L}^{-1})$	
	ADP ($10\ \mu\text{mol}\cdot\text{L}^{-1}$)	AA ($1\ \text{mmol}\cdot\text{L}^{-1}$)
6h	0.12 \pm 0.04	0.07 \pm 0.01
TMP	1.27 \pm 0.22	0.79 \pm 0.14
RES	0.62 \pm 0.04	0.52 \pm 0.03
TMP + RES (1 : 1)	0.34 \pm 0.01	0.22 \pm 0.01
TMP + RES (1 : 2)	0.25 \pm 0.01	0.19 \pm 0.01

tion was weaker than that of 6h. Moreover, the inhibition of 6h was significantly more potent than that of TMP and RES in combination (1 : 1 and 1 : 2, respectively). These results indicated that both RES and TMP moieties in 6h may possess synergistic effects on anti-platelet aggregation activity.

In vitro antioxidant activity assay

It is well-known that ischemic tissues would suffer fatal oxidative damages after reperfusion [29, 30]. Therefore, we evaluated the antioxidative effect of 6h on rat pheochromocytoma PC12 cells which were treated with hydrogen peroxide (H₂O₂) or hydroxyl radicals (·OH). As can be seen from Fig. 1, H₂O₂ or ·OH displayed obvious cell damage effect on PC12 cells after incubation for 1 h, and the cell viability was reduced by 52.52% and 58.20%, respectively. However, the cell viability by pretreatment with 6h at 10 μmol·L⁻¹ was improved to be 72.59% and 80.59%, respectively, which is more potent than that of TMP (62.15% and 70.16%) or RES (59.88% and 64.25%) pretreatment under the same conditions. Additionally, the cell viability of PC12 cells which were pretreated with RES (10 μmol·L⁻¹) plus TMP (10 μmol·L⁻¹) was 66.19% and 74.20%, respectively. When the concentration of RES was increased to 20 μmol·L⁻¹ (TMP : RES, 1 : 2), the viability was only slightly up to 68.32% and 79.63%. Notably, the viability of 6h was somewhat greater than a known clinic drug edaravone (Eda) (71.42% and 79.50%) under the same conditions. Collectively, 6h exhibited the most potent protective activity among all tested groups.

Oxygen-glucose deprivation (OGD) and recovery (R) induction

We further investigated the effects of 6h on primary neuronal cells survival rate in an oxygen-glucose deprivation/reoxygenation (OGD/R) model, which is used for simulating cerebral ischemia/reperfusion *in vitro*. As shown in Fig. 2, in comparison with control group, the neuron survival rate of OGD/R group was significantly reduced. All tested groups improved the survival rate of neurons relative to the model group. The neuroprotective effect of 6h (1

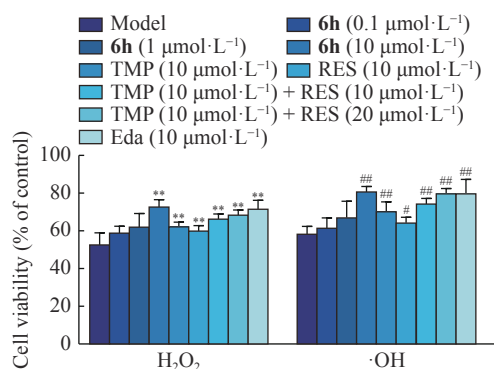


Fig. 1 Protection from H₂O₂- or ·OH-induced cytotoxicity in PC12 cells. Data are expressed as the mean ± SD of each group from five separate experiment and are analyzed by one-way analysis of variance (ANOVA) followed by post hoc Tukey test. **P < 0.01 vs the H₂O₂-treated group; #P < 0.05, ###P < 0.01 vs the ·OH-treated group

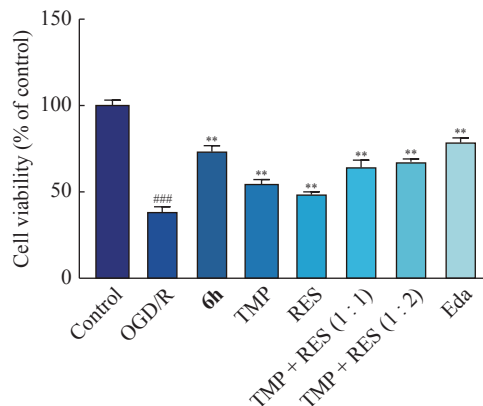


Fig. 2 Effects of the test compounds (1 μmol·L⁻¹) on the survive rate of primary rat hippocampal neurons treated by oxygen/glucose deprivation and reoxygenation. Data are expressed as the mean ± SD of each group from five separate experiment and are analyzed by one-way analysis of variance (ANOVA) followed by post hoc Tukey test. **P < 0.01 vs OGD/R group; ###P < 0.001 vs control group

μmol·L⁻¹) was better than that of TMP and RES alone or in combination (1 : 1 or 1 : 2) and comparable to Eda. All the data above indicates that 6h had a significant protective effect on OGD/R-induced neuronal damage, and possibly thanks to the synergistic effects of each moiety in 6h.

Experimental

Chemistry

General experimental procedures

Melting points of individual compounds were determined on a Mel-TEMP II melting point apparatus and uncorrected. ¹H NMR and ¹³C NMR spectra were recorded with a Bruker Avance 300 MHz spectrometer at 303 K, using TMS as an internal standard. Mass spectra were obtained on an Agilent Q-TOF 6540 spectrometer. All compounds were routinely checked by TLC and ¹H NMR. TLC were performed on silica gel GF/UV 254, and the chromatograms were conducted on silica gel (200–300 mesh) and visualized under UV light at 254 or 365 nm. All solvents were reagent grade and, when necessary, were purified and dried by standard methods. Solutions after reactions and extractions were concentrated using a rotary evaporator operating at a reduced pressure of ca. 20 Torr. The purity of all tested compounds was characterized by HPLC analysis (Shimadzu LC-20A HPLC system consisting of LC-20AT pumps and an SPD-20AV UV detector).

General procedure for the preparation of 2

To a stirred solution of TMP hydrochloride (41.5 g, 200 mmol) in H₂O (400 mL), NaOH (8 g, 200 mmol) in 50 mL H₂O was added dropwise at 0 °C, and the mixture was stirred at room temperature for 2 h. Then the precipitate was collected by filtration and dried to give ligustrazine trihydrate. Next, to the solution of ligustrazine trihydrate (38 g, 200 mmol) in glacial acetic acid (45 mL), 30% H₂O₂ (36 mL, 320 mmol) aqueous solution was added. After stirring at 95 °C for 18 h, another portion of 30% H₂O₂ (36 mL, 320 mmol) was

added and heated at reflux for 4 h. The resulted mixture was alkalized to pH 10 with 20% NaOH (aq) and extracted with trichloromethane. Combined organic layer was washed with brine, dried over anhydrous sodium sulfate and concentrated in vacuo to afford crude product **1**, which was used without further purification.

Compound **1** was then dissolved in acetic anhydride and stirred at reflux for 2.5 h. The acetic anhydride was removed in vacuo and purified by column chromatography to get **2** as a yellow solid, yield 67%. ¹H NMR (300 MHz, CDCl₃) δ: 5.22 (s, 4H), 2.57 (s, 6H), 2.13 (s, 6H). ¹³C NMR (300 MHz, CDCl₃) δ: 170.51, 149.42, 147.38, 64.73, 20.68, 20.53. ESI-MS *m/z* 253.1 ([M + H]⁺).

General procedure for the preparation of **3**

A solution of compound **2** in 20% NaOH (aq) (300 mL) was stirred at room temperature overnight. The reaction mixture was extracted with trichloromethane. Combined organic layer was washed with H₂O, brine, dried over anhydrous sodium sulfate and concentrated in vacuo, then recrystallization with petroleum ether to afford **3** as a yellow needle crystal, yield 32%. Melting point 110–112 °C. ¹H NMR (300 MHz, CDCl₃) δ: 7.27 (s, 4H), 2.58 (s, 2H), 2.48 (s, 6H). ¹³C NMR (300 MHz, CDCl₃) δ: 149.15, 149.25, 147.18, 146.17, 60.47, 61.05, 21.21, 19.21. ESI-MS *m/z* 169.3 ([M + H]⁺).

General procedure for the preparation of **4**

To a solution of compound **3** (1.68 g, 10.0 mmol, 1.0 eq) in CH₂Cl₂, phosphorus tribromide (0.95 mL, 10.0 mmol, 1.0 eq) was added dropwise, and the mixture was stirred in an ice bath for 0.5 h. The reaction solution was quenched with saturated Na₂CO₃ solution, then the pH was adjusted to 7 with 10% acetic acid and extracted with CH₂Cl₂. The organic layer was collected, washed with brine, and dried over anhydrous sodium sulfate. Remove the solvent and compound **4** was obtained as a yellow solid. The crude product **4** was directly used in the following step without further purification.

General procedure for the preparation of **5**

A solution of compound **4** (2.69 g, 9.2 mmol, 1.0 eq) in triethylphosphite (20 mL) was heat at reflux for 1 h. After completion of the reaction, the solvent was removed by evaporation in vacuo and the residue was then purified by column chromatography to provide **5** as yellow solid, yield 67%. ¹H NMR (300 MHz, CDCl₃) δ: 4.19–4.02 (m, 8H), 3.39 (d, *J* = 20.9 Hz, 4H), 2.58 (s, 6H), 1.28 (t, *J* = 7.1 Hz, 12H).

General procedure for the preparation of **6a–6t**

To a stirred solution of compound **5** (122.4 mg, 0.3 mmol, 1.0 eq) in anhydrous THF was added NaH (28 mg, 0.75 mmol, 2.5 eq) in an ice bath for 0.5 h. Then the individual substituted benzaldehydes (0.75 mmol, 2.5 eq) were added. After completion of the reaction, the reaction was quenched by water and extracted with CH₂Cl₂. The organic layer was collected and dried over anhydrous sodium sulfate. The solvent was removed under vacuum and the resulted residue was purified by column chromatography to afford corresponding **6a–6t**.

2, 5-Dimethyl-3, 6-di((E)-styryl) pyrazine (**6a**)

The title compound **6a** was obtained starting from **5** and

benzaldehyde (79.6 mg, 0.75 mmol, 2.5 eq) as a yellowish solid. Yield 65%. Melting point 296–298 °C. ¹H NMR (300 MHz, CDCl₃) δ: 7.76 (d, *J* = 15.7 Hz, 2H), 7.63 (d, *J* = 10.1 Hz, 4H), 7.43–7.28 (m, 8H), 2.70 (s, 6H). ¹³C NMR (75 MHz, CDCl₃) δ: 148.08, 146.09, 136.92, 134.65, 128.72, 128.48, 127.28, 122.84, 21.39. ESI-MS *m/z* 311.2 ([M – H][−]).

2, 5-Bis((E)-3, 4-dimethoxystyryl)-3, 6-dimethylpyrazine (**6b**)

The title compound **6b** was obtained starting from **5** and 3, 4-dimethoxybenzaldehyde (124.6 mg, 0.75 mmol, 2.5 eq) as a yellowish solid. Yield 57%. Melting point 265–267 °C. ¹H NMR (300 MHz, CDCl₃) δ: 7.77 (d, *J* = 15.4 Hz, 2H), 7.21–7.14 (m, 6H), 6.89 (d, *J* = 8.3 Hz, 2H), 3.96 (s, 6H), 3.93 (s, 6H), 2.70 (s, 6H). ¹³C NMR (75 MHz, CDCl₃) δ: 149.85, 149.21, 147.69, 134.70, 130.07, 120.91, 120.67, 118.84, 111.33, 109.88, 55.98, 21.39. ESI-MS *m/z* 432.2 ([M]⁺).

4, 4'-((1E, 1'E)-(3, 6-Dimethylpyrazine-2, 5-diyl)bis(ethene-2, 1-diyl))bis(2-methoxyphenol) (**6c**)

The title compound **6c** was obtained starting from **5** and 4-hydroxy-3-methoxybenzaldehyde (114.1 mg, 0.75 mmol, 2.5 eq) as a yellowish solid. Yield 45%. Melting point 256–258 °C. ¹H NMR (300 MHz, DMSO-*d*₆) δ: 9.33 (s, 2H), 7.64 (d, *J* = 15.5 Hz, 2H), 7.32 (s, 2H), 7.25 (d, *J* = 15.8 Hz, 2H), 7.15 (d, *J* = 8.2 Hz, 2H), 6.80 (d, *J* = 8.1 Hz, 2H), 3.86 (s, 6H), 2.63 (s, 6H). ¹³C NMR (75 MHz, DMSO-*d*₆) δ: 147.82, 147.56, 147.28, 145.30, 133.91, 128.15, 121.09, 119.83, 115.61, 110.96, 55.71, 21.04. ESI-MS *m/z* 405.2 ([M + H]⁺).

2, 5-Dimethyl-3, 6-bis((E)-3, 4, 5-trimethoxystyryl)pyrazine (**6d**)

The title compound **6d** was obtained starting from **5** and 3, 4, 5-trimethoxybenzaldehyde (147.2 mg, 0.75 mmol, 2.5 eq) as a yellowish solid. Yield 60%. Melting point 267–269 °C. ¹H NMR (300 MHz, CDCl₃) δ: 7.76 (d, *J* = 15.5 Hz, 2H), 7.18 (d, *J* = 15.5 Hz, 2H), 6.84 (s, 4H), 3.94 (s, 12H), 3.89 (s, 6H), 2.70 (s, 6H). ¹³C NMR (75 MHz, CDCl₃) δ: 153.47, 147.93, 145.92, 139.02, 138.60, 134.94, 132.52, 122.04, 104.65, 60.98, 56.24, 21.43. ESI-MS *m/z* 515.2 ([M + Na]⁺).

2, 5-bis((E)-4-Methoxystyryl)-3, 6-dimethylpyrazine (**6e**)

The title compound **6e** was obtained starting from **5** and 4-methoxybenzaldehyde (102.1 mg, 0.75 mmol, 2.5 eq) as a yellowish solid. Yield 60%. Melting point 239–241 °C. ¹H NMR (300 MHz, CDCl₃) δ: 7.77 (d, *J* = 15.5 Hz, 2H), 7.56 (d, *J* = 8.2 Hz, 4H), 7.16 (d, *J* = 15.5 Hz, 2H), 6.92 (d, *J* = 8.2 Hz, 4H), 3.85 (s, 6H), 2.67 (s, 6H). ¹³C NMR (75 MHz, CDCl₃) δ: 160.04, 147.72, 146.02, 134.05, 129.83, 128.65, 120.68, 114.22, 55.33, 21.41. ESI-MS *m/z* 373.2 ([M + H]⁺).

2, 5-bis((E)-2-Methoxystyryl)-3, 6-dimethylpyrazine (**6f**)

The title compound **6f** was obtained starting from **5** and 3-bromo-4-methoxybenzaldehyde (161.3 mg, 0.75 mmol, 2.5 eq) as a yellowish solid. Yield 55%. Melting point 245–247 °C. ¹H NMR (300 MHz, CDCl₃) δ: 7.82 (d, *J* = 12.1 Hz, 2H), 7.72 (d, *J* = 15.6 Hz, 2H), 7.49 (d, *J* = 8.5 Hz, 2H), 7.15 (d, *J* = 15.6 Hz, 2H), 6.91 (d, *J* = 8.4 Hz, 2H), 3.93 (s, 6H), 2.68 (s, 6H). ¹³C NMR (75 MHz, CDCl₃) δ: 157.58, 147.85,

145.74, 131.54, 128.14, 127.39, 125.59, 124.72, 121.83, 111.89, 56.35, 21.45.

2, 5-bis((E)-2-Methoxystyryl)-3, 6-dimethylpyrazine (6g)

The title compound **6g** was obtained starting from **5** and 2-methoxybenzaldehyde (102.1 mg, 0.75 mmol, 2.5 eq) as a yellowish solid. Yield 67%. Melting point 218–220 °C. ¹H NMR (300 MHz, CDCl₃) δ: 8.10 (d, *J* = 15.8 Hz, 2H), 7.63 (d, *J* = 7.6 Hz, 2H), 7.38 (d, *J* = 15.7 Hz, 2H), 7.35–7.29 (m, 2H), 7.01–6.92 (m, 4H), 3.93 (s, 6H), 2.69 (s, 6H). ¹³C NMR (75 MHz, CDCl₃) δ: 157.72, 148.03, 146.43, 129.72, 129.44, 127.82, 126.16, 123.95, 120.67, 111.00, 55.48, 21.44. ESI-MS *m/z* 373.2 ([M + H]⁺).

4, 4'-((1E, 1'E)-(3, 6-Dimethylpyrazine-2, 5-diyl)bis(ethene-2, 1-diyl)diphenol (6h)

The title compound **6h** was obtained starting from **5** and 4-hydroxybenzaldehyde (91.2 mg, 0.75 mmol, 2.5 eq) as a yellowish solid. Yield 43%. Melting point > 300 °C. ¹H NMR (300 MHz, DMSO-*d*₆) δ: 9.75 (s, 2H), 7.62 (d, *J* = 15.8 Hz, 2H), 7.56 (d, *J* = 8.2 Hz, 4H), 7.21 (d, *J* = 15.5 Hz, 2H), 6.80 (d, *J* = 7.9 Hz, 4H), 2.61 (s, 6H). ¹³C NMR (75 MHz, DMSO-*d*₆) δ: 158.58, 148.79, 145.80, 131.30, 129.34, 128.11, 120.11, 116.09, 21.50. ESI-MS *m/z* 345.1 ([M + H]⁺).

2, 2'-((1E, 1'E)-(3, 6-Dimethylpyrazine-2, 5-diyl)bis(ethene-2, 1-diyl)diphenol (6i)

The title compound **6i** was obtained starting from **5** and 2-hydroxybenzaldehyde (91.2 mg, 0.75 mmol, 2.5 eq) as a yellowish solid. Yield 46%. Melting point 242–244 °C. ¹H NMR (300 MHz, DMSO-*d*₆) δ: 9.95 (s, 2H), 8.01 (d, *J* = 15.6 Hz, 2H), 7.73 (d, *J* = 8.1 Hz, 2H), 7.49 (d, *J* = 15.5 Hz, 2H), 7.16–7.12 (m, 2H), 6.92–6.82 (m, 4H), 2.63 (s, 6H). ¹³C NMR (75 MHz, DMSO-*d*₆) δ: 155.74, 147.61, 145.69, 129.52, 129.17, 127.39, 123.40, 122.13, 119.32, 115.94, 21.07. ESI-MS *m/z* 345.2 ([M + H]⁺).

2, 5-Dimethyl-3, 6-bis((E)-4-methylstyryl) pyrazine (6j)

The title compound **6j** was obtained starting from **5** and 4-methylbenzaldehyde (90.1 mg, 0.75 mmol, 2.5 eq) as a yellowish solid. Yield 66%. Melting point 223–225 °C. ¹H NMR (300 MHz, CDCl₃) δ: 7.79 (d, *J* = 15.6 Hz, 2H), 7.51 (d, *J* = 7.8 Hz, 4H), 7.28–7.18 (m, 6H), 2.68 (s, 6H), 2.38 (s, 6H). ¹³C NMR (75 MHz, CDCl₃) δ: 147.90, 146.07, 138.52, 134.47, 129.43, 128.27, 127.20, 121.89, 21.39, 21.31.

2, 5-Dimethyl-3, 6-bis((E)-3-methylstyryl) pyrazine (6k)

The title compound **6k** was obtained starting from **5** and 3-methylbenzaldehyde (90.1 mg, 0.75 mmol, 2.5 eq) as a yellowish solid. Yield 72%. Melting point 195–197 °C. ¹H NMR (300 MHz, CDCl₃) δ: 7.80 (d, *J* = 15.6 Hz, 2H), 7.42 (d, *J* = 8.2 Hz, 4H), 7.31–7.28 (m, 4H), 7.13 (d, *J* = 7.5 Hz, 2H), 2.69 (s, 6H), 2.40 (s, 6H). ¹³C NMR (75 MHz, CDCl₃) δ: 148.00, 146.08, 138.26, 136.86, 134.79, 129.33, 128.60, 127.89, 124.53, 122.61, 21.38.

2, 5-Dimethyl-3, 6-bis((E)-2-methylstyryl) pyrazine (6l)

The title compound **6l** was obtained starting from **5** and 2-methylbenzaldehyde (90.1 mg, 0.75 mmol, 2.5 eq) as a yellowish solid. Yield 69%. Melting point 203–205 °C. ¹H NMR (300 MHz, CDCl₃) δ: 8.07 (d, *J* = 15.5 Hz, 2H), 7.69–7.66 (m, 2H), 7.26–7.18 (m, 8H), 2.69 (s, 6H), 2.51 (s, 6H). ¹³C

NMR (75 MHz, CDCl₃) δ: 148.05, 146.25, 136.82, 136.01, 132.68, 130.55, 128.34, 126.15, 125.80, 124.06, 21.39, 19.96.

2, 5-bis((E)-2-Chlorostyryl)-3, 6-dimethylpyrazine (6m)

The title compound **6m** was obtained starting from **5** and 2-chlorobenzaldehyde (105.4 mg, 0.75 mmol, 2.5 eq) as a yellowish solid. Yield 45%. Melting point 249–250 °C. ¹H NMR (300 MHz, CDCl₃) δ: 8.20 (d, *J* = 15.6 Hz, 2H), 7.74 (dd, *J* = 7.6, 1.8 Hz, 2H), 7.43 (dd, *J* = 7.5, 1.4 Hz, 2H), 7.44–7.22 (m, 6H), 2.71 (s, 6H). ¹³C NMR (75 MHz, CDCl₃) δ: 148.40, 146.14, 135.12, 134.27, 131.17, 130.00, 129.34, 127.13, 126.90, 125.54, 21.39.

2, 5-bis((E)-4-Chlorostyryl)-3, 6-dimethylpyrazine (6n)

The title compound **6n** was obtained starting from **5** and 4-chlorobenzaldehyde (105.4 mg, 0.75 mmol, 2.5 eq) as a yellowish solid. Yield 43%. Melting point 282–284 °C. ¹H NMR (300 MHz, CDCl₃) δ: 7.78 (d, *J* = 15.7 Hz, 2H), 7.54 (d, *J* = 8.4 Hz, 4H), 7.36 (d, *J* = 8.4 Hz, 4H), 7.27 (d, *J* = 15.5 Hz, 2H), 2.69 (s, 6H). ¹³C NMR (75 MHz, CDCl₃) δ: 153.91, 144.58, 137.83, 134.91, 133.00, 128.50, 127.97, 122.80, 76.94, 76.51, 76.09, 20.87.

2, 5-bis((E)-4-Bromostyryl)-3, 6-dimethylpyrazine (6o)

The title compound **6o** was obtained starting from **5** and 4-bromobenzaldehyde (138.8 mg, 0.75 mmol, 2.5 eq) as a yellowish solid. Yield 38%. Melting point 284–286 °C. ¹H NMR (300 MHz, CDCl₃) δ: 7.77 (d, *J* = 15.6 Hz, 2H), 7.52–7.46 (m, 8H), 7.28 (d, *J* = 15.4 Hz, 2H), 2.69 (s, 6H). ¹³C NMR (75 MHz, CDCl₃) δ: 148.18, 145.86, 134.12, 131.93, 131.34, 130.40, 128.76, 122.86, 21.18.

2, 5-bis((E)-3-Methoxystyryl)-3, 6-dimethylpyrazine (6p)

The title compound **6p** was obtained starting from **5** and 3-methoxybenzaldehyde (102.1 mg, 0.75 mmol, 2.5 eq) as a yellowish solid. Yield 38%. Melting point 184–186 °C. ¹H NMR (300 MHz, CDCl₃) δ: 7.80 (d, *J* = 15.6 Hz, 2H), 7.33–7.23 (m, 6H), 7.15–7.12 (m, 2H), 6.89–6.85 (m, 2H), 3.86 (s, 6H), 2.69 (s, 6H). ¹³C NMR (75 MHz, CDCl₃) δ: 159.91, 148.10, 146.00, 138.30, 134.82, 129.67, 122.97, 119.94, 114.20, 112.67, 55.28, 21.32. ESI-MS *m/z* 373.2 ([M + H]⁺).

3, 3'-((1E, 1'E)-(3, 6-Dimethylpyrazine-2, 5-diyl)bis(ethene-2, 1-diyl)diphenol (6q)

The title compound **6q** was obtained starting from **5** and 3-hydroxybenzaldehyde (91.6 mg, 0.75 mmol, 2.5 eq) as a yellowish solid. Yield 42%. Melting point > 300 °C. ¹H NMR (300 MHz, DMSO-*d*₆) δ: 9.50 (s, 2H), 7.64 (d, *J* = 15.5 Hz, 2H), 7.36 (d, *J* = 15.6 Hz, 2H), 7.21–7.17 (m, 4H), 7.09 (s, 2H), 6.77–6.74 (m, 2H), 2.65 (s, 6H). ¹³C NMR (75 MHz, DMSO-*d*₆) δ: 157.62, 147.88, 145.36, 137.65, 133.92, 129.67, 122.72, 118.45, 115.79, 113.60, 20.96. ESI-MS *m/z* 345.2 ([M + H]⁺).

2, 5-bis((E)-2, 4-Dimethoxystyryl)-3, 6-dimethylpyrazine (6r)

The title compound **6r** was obtained starting from **5** and 2, 4-dimethoxybenzaldehyde (124.6 mg, 0.75 mmol, 2.5 eq) as a yellowish solid. Yield 50%. Melting point 279–281 °C. ¹H NMR (300 MHz, CDCl₃) δ: 8.00 (d, *J* = 15.7 Hz, 2H), 7.55 (d, *J* = 8.5 Hz, 2H), 7.28 (d, *J* = 15.7 Hz, 2H), 6.55–6.48 (m, 4H), 3.91 (s, 6H), 3.85 (s, 6H), 2.66 (s, 6H). ¹³C NMR

(75 MHz, CDCl₃) δ: 159.06, 151.83, 148.22, 141.86, 129.12, 127.91, 121.15, 108.68, 105.09, 98.51, 55.49, 55.39. ESI-MS *m/z* 433.2 ([M + H]⁺).

4, 4'-((1*E*, 1'*E*)-(3, 6-Dimethylpyrazine-2, 5-diyl)bis(ethene-2, 1-diyl))bis(*N*, *N*-dimethylaniline) (**6s**)

The title compound **6s** was obtained starting from **5** and 4-(dimethyl amino) benzaldehyde (111.9 mg, 0.75 mmol, 2.5 eq) as a yellowish solid. Yield 52%. Melting point 271–273 °C. ¹H NMR (300 MHz, CDCl₃) δ: 7.73 (d, *J* = 15.5 Hz, 2H), 7.51 (d, *J* = 8.7 Hz, 4H), 7.08 (d, *J* = 15.5 Hz, 2H), 6.71 (d, *J* = 8.7 Hz, 4H), 3.00 (s, 12H), 2.65 (s, 6H). ¹³C NMR (75 MHz, CDCl₃) δ: 150.54, 147.34, 145.97, 134.14, 128.51, 125.51, 118.53, 112.24, 40.32, 21.50. ESI-MS *m/z* 399.2 ([M + H]⁺).

2, 5-bis(*E*)-4-Fluorostyryl)-3, 6-dimethylpyrazine (**6t**)

The title compound **6t** was obtained starting from **5** and 4-fluorobenzaldehyde (93.1 mg, 0.75 mmol, 2.5 eq) as a yellowish solid. Yield 63%. Melting point 282–284 °C. ¹H NMR (300 MHz, CDCl₃) δ: 7.79 (d, *J* = 15.6 Hz, 2H), 7.67–7.56 (m, 4H), 7.21 (d, *J* = 15.7 Hz, 2H), 7.08 (t, *J* = 8.6 Hz, 4H), 2.68 (s, 6H). ¹³C NMR (75 MHz, CDCl₃) δ: 164.56, 147.99, 145.94, 133.64, 133.08, 128.95, 128.84, 122.36, 115.89, 115.61, 21.29. ESI-MS *m/z* 347.1 ([M – H][−]).

Biological evaluation

Anti-platelet aggregation *in vitro* ^[31]

Blood samples were withdrawn from rabbit carotid artery and mixed with 3.8% sodium citrate (9 : 1, *V/V*). After centrifugation at 1000 r·min^{−1} for 15 min at room temperature to obtain PRP, the remaining blood was further centrifuged at 3000 r·min^{−1} for another 15 min to obtain platelet-poor plasma (PPP). Platelet aggregation was measured by Born's turbidimetric method in a platelet aggregometer (LG-PABER-I platelet aggregometer, Beijing, China) at 37 °C within 3 h after blood collection. Briefly, PRP (260 μL) was preincubated in duplicate for 5 min at 37 °C with vehicle, the individual compounds, or reference drugs (ASP and Ticlid) at the same concentrations (0.01, 0.05, 0.1, 0.5 and 1 mmol·L^{−1}) and the platelet aggregation in individual PPR samples was induced by ADP (final concentration of 10 μmol·L^{−1}) or AA (final concentration of 1 mmol·L^{−1}), followed by recording of light transmission at maximal aggregation within 5 min. The inhibition rate of the tested individual compounds on the platelet aggregation was calculated as the following formula: inhibition rate (%) = 100 × [(1 – (the platelet aggregation in samples with the tested compound)/(the platelet aggregation in control samples)]. In addition, the concentrations of selected compounds that inhibited the platelet aggregation to 50% (IC₅₀) were calculated.

In vitro antioxidant activity assay ^[32]

Cell culture and treatment

PC12 cells were cultured in DMEM supplemented with 10% (*V/V*) heat-inactivated fetal bovine serum, 5% FBS, 1 mmol·L^{−1} sodium pyruvate, 100 U·mL^{−1} penicillin and 100 μg·mL^{−1} streptomycin in a humidified atmosphere of 5% CO₂/95% air at 37 °C in poly-lysine-coated flasks.

For all experiments, the cells were used at logarithmic

phase and seeded at a concentration of 1 × 10⁵ cells/mL. The cells were incubated with individual compounds in 1% FBS–DMEM medium for 2 h, respectively, and then incubated for 1 h in 1% FBS–DMEM medium containing 800 μmol·L^{−1} H₂O₂ or 1 mmol·L^{−1} H₂O₂/20 μmol·L^{−1} Fe²⁺ (pH 7.4). And then, incubation was continued for 14 h using 1% FBS–DMEM medium without H₂O₂.

Cell viability measurement by MTT assay

Cell viability was measured by the MTT assay. Briefly, after exposure to H₂O₂, 20 μL of MTT dye was added to each well at a final concentration of 5 mg·mL^{−1}. After 4 h of incubation, 150 μL of DMSO, the solubilization/stop solution, was added to dissolve the formazan crystals, and the absorbance was read using a microtiter plate reader at a wavelength of 570 nm.

Oxygen-glucose deprivation (OGD) and recovery (R) induction ^[33]

The rat cortical neurons were isolated as described previously. Generally, SD rat embryos at E18–E19 were obtained from Experimental Animal Center of Nanjing University, Nanjing, China and sacrificed by cervical dislocation under general anesthesia. Their brain cortex tissues were dissected out and mechanically and enzymatically dissociated to prepare single cell suspensions. Primary cortical neurons (4 × 10⁴ cells/mL) were cultured onto poly-lysine-coated plates in DMEM supplemented with 10% FBS for 4 h at 37 °C in a humidified atmosphere of 95% air and 5% CO₂ to allow cell adhesion. The primary cortical neurons were pretreated with corresponding compounds (1 μmol·L^{−1}) in primary Neuron Basal Medium with 2% B27 supplement (Invitrogen) for 24 h. After being washed, the cells were cultured in glucose- and FBS-free DMEM in 1% O₂, 5% CO₂, and 94% N₂ for 2 h at 37 °C to induce OGD injury. Subsequently, the cells were cultured in 10% FBS–DMEM (5% glucose) for 24 h at 37 °C in a humidified atmosphere of 20% O₂ and 5% CO₂. The cell viability was measured by MTT assay.

Conclusions

In summary, a series of TMP/RES hybrids **6a–t** were designed, synthesized and biologically evaluated. The most potent compound **6h** displayed excellent anti-platelet aggregative and antioxidative activities, and improved OGD/R primary neuronal cell viability, which were superior to TMP, RES and/or other clinical drug(s), deserving further investigations for the treatment of ischemic stroke.

Abbreviations

AA, arachidonic acid; ADP, adenosine diphosphate; ASP, aspirin; eNOS, endothelial nitric oxide synthase; H₂O₂, hydrogen peroxide; iNOS, inducible nitric oxide synthase; MCAO, middle cerebral artery occlusion; NLRP-3, pyrin domain-containing 3 inflammasome; NPCs, neuronal precursor cells; OGD/R, oxygen-glucose deprivation/reoxygenation; ·OH, hydroxyl radical; PPP, platelet-poor plasma; PRP, platelet-rich plasma; RES, resveratrol; SARs, structure-activity relationships; TBN, tetramethylpyrazine nitron; Ticlid, ticlopidin.

idine hydrochloride; TMP, 2, 3, 5, 6-tetramethylpyrazine, ligustrazine.

References

- [1] Global, regional, and national life expectancy, all-cause mortality, and cause-specific mortality for 249 causes of death, 1980-2015: a systematic analysis for the Global Burden of Disease Study 2015 [J]. *Lancet*, 2016, **388**(10053): 1459-1544.
- [2] Mozaffarian D, Benjamin EJ, Go AS, et al. Heart disease and stroke statistics-2016 update: A report from the American heart association [J]. *Circulation*, 2016, **133**(4): e38-360.
- [3] Wang W, Jiang B, Sun H, et al. Prevalence, incidence, and mortality of stroke in China: results from a nationwide population-based survey of 480 687 adults [J]. *Circulation*, 2017, **135**(8): 759-771.
- [4] Doyle KP, Simon RP, Stenzel-Poore MP. Mechanisms of ischemic brain damage [J]. *Neuropharmacology*, 2008, **55**(3): 310-318.
- [5] Haraoui B, Liu PP, Papp KA. Managing cardiovascular risk in patients with chronic inflammatory diseases [J]. *Clin Rheumatol*, 2012, **31**(4): 585-594.
- [6] Atiquzzaman M, Karim ME, Kopec J, et al. Role of nonsteroidal antiinflammatory drugs in the association between osteoarthritis and cardiovascular diseases: a longitudinal study [J]. *Arthritis Rheumatol*, 2019, **71**(11): 1835-1843.
- [7] Cai W, Wang J, Hu M, et al. All trans-retinoic acid protects against acute ischemic stroke by modulating neutrophil functions through STAT1 signaling [J]. *J Neuroinflammation*, 2019, **16**(1): 175.
- [8] Hackam DG, Spence JD. Antiplatelet therapy in ischemic stroke and transient ischemic attack [J]. *Stroke*, 2019, **50**(3): 773-778.
- [9] Macha K, Marsch A, Siedler G, et al. Cerebral ischemia in patients on direct oral anticoagulants [J]. *Stroke*, 2019, **50**(4): 873-879.
- [10] Amaro S, Laredo C, Renu A, et al. Uric acid therapy prevents early ischemic stroke progression: a tertiary analysis of the URICO-ICTUS trial (efficacy study of combined treatment with uric acid and r-tpa in acute ischemic stroke) [J]. *Stroke*, 2016, **47**(11): 2874-2876.
- [11] Broderick JP, Bonomo JB, Kissela BM, et al. Withdrawal of antithrombotic agents and its impact on ischemic stroke occurrence [J]. *Stroke*, 2011, **42**(9): 2509-2514.
- [12] Jiang X, Andjelkovic AV, Zhu L, et al. Blood-brain barrier dysfunction and recovery after ischemic stroke [J]. *Prog Neurobiol*, 2018, **163-164**: 144-171.
- [13] Tian Y, Liu Y, Chen X, et al. Tetramethylpyrazine promotes proliferation and differentiation of neural stem cells from rat brain in hypoxic condition via mitogen-activated protein kinases pathway *in vitro* [J]. *Neurosci Lett*, 2010, **474**(1): 26-31.
- [14] Xiao X, Liu Y, Qi C, et al. Neuroprotection and enhanced neurogenesis by tetramethylpyrazine in adult rat brain after focal ischemia [J]. *Neurol Res*, 2010, **32**(5): 547-555.
- [15] Kong X, Zhong M, Su X, et al. Tetramethylpyrazine promotes migration of neural precursor cells via activating the phosphatidylinositol 3-kinase pathway [J]. *Mol Neurobiol*, 2016, **53**(9): 6526-6539.
- [16] Sun Y, Jiang J, Zhang Z, et al. Antioxidative and thrombolytic TMP nitron for treatment of ischemic stroke [J]. *Bioorg Med Chem*, 2008, **16**(19): 8868-8874.
- [17] Sun Y, Yu P, Zhang G, et al. Therapeutic effects of tetramethylpyrazine nitron in rat ischemic stroke models [J]. *J Neurosci Res*, 2012, **90**(8): 1662-1669.
- [18] Zhang Z, Zhang G, Sun Y, et al. Tetramethylpyrazine nitron, a multifunctional neuroprotective agent for ischemic stroke therapy [J]. *Sci Rep*, 2016, **6**: 37148.
- [19] Shin NH, Ryu SY, Lee H, et al. Inhibitory effects of hydroxystilbenes on cyclooxygenase from sheep seminal vesicles [J]. *Planta Med*, 1998, **64**(3): 283-284.
- [20] Bertelli AA, Giovannini L, Giannessi D, et al. Antiplatelet activity of synthetic and natural resveratrol in red wine [J]. *Int J Tissue React*, 1995, **17**(1): 1-3.
- [21] Tsai SK, Hung LM, Fu YT, et al. Resveratrol neuroprotective effects during focal cerebral ischemia injury via nitric oxide mechanism in rats [J]. *J Vasc Surg*, 2007, **46**(2): 346-353.
- [22] Fang L, Gao H, Zhang W, et al. Resveratrol alleviates nerve injury after cerebral ischemia and reperfusion in mice by inhibiting inflammation and apoptosis [J]. *Int J Clin Exp Med*, 2015, **8**(3): 3219-3226.
- [23] Kizmazoglu C, Aydin HE, Sevin IE, et al. Neuroprotective effect of resveratrol on acute brain ischemia reperfusion injury by measuring annexin V, p53, Bcl-2 levels in rats [J]. *J Korean Neurosurg Soc*, 2015, **58**(6): 508-512.
- [24] He Q, Li Z, Wang Y, et al. Resveratrol alleviates cerebral ischemia/reperfusion injury in rats by inhibiting NLRP3 inflammasome activation through Sirt1-dependent autophagy induction [J]. *Int Immunopharmacol*, 2017, **50**: 208-215.
- [25] Koronowski KB, Dave KR, Saul I, et al. Resveratrol preconditioning induces a novel extended window of ischemic tolerance in the mouse brain [J]. *Stroke*, 2015, **46**(8): 2293-2298.
- [26] Narayanan SV, Dave KR, Saul I, et al. Resveratrol preconditioning protects against cerebral ischemic injury via nuclear erythroid 2-related factor 2 [J]. *Stroke*, 2015, **46**(6): 1626-1632.
- [27] Jacobson AK. Platelet ADP receptor antagonists: ticlopidine and clopidogrel [J]. *Best Pract Res Clin Haematol*, 2004, **17**(1): 55-64.
- [28] Caso V, Santalucia P, Acciarresi M, et al. Antiplatelet treatment in primary and secondary stroke prevention in women [J]. *Eur J Intern Med*, 2012, **23**(7): 580-585.
- [29] Van Zandt MC, Whitehouse DL, Golebiowski A, et al. Discovery of (R)-2-amino-6-borono-2-(2-(piperidin-1-yl)ethyl)hexanoic acid and congeners as highly potent inhibitors of human arginases I and II for treatment of myocardial reperfusion injury [J]. *J Med Chem*, 2013, **56**(6): 2568-2580.
- [30] Rodrigo R, Fernandez-Gajardo R, Gutierrez R, et al. Oxidative stress and pathophysiology of ischemic stroke: novel therapeutic opportunities [J]. *CNS Neurol Disord Drug Targets*, 2013, **12**(5): 698-714.
- [31] Born GV, Cross MJ. The aggregation of blood platelets [J]. *J Physiol*, 1963, **168**: 178-195.
- [32] Zhai L, Zhang P, Sun RY, et al. Cytoprotective effects of CST-MP, a novel stilbene derivative, against H₂O₂-induced oxidative stress in human endothelial cells [J]. *Pharmacol Rep*, 2011, **63**(6): 1469-1480.
- [33] Agrawal M, Kumar V, Singh AK, et al. trans-Resveratrol protects ischemic PC12 Cells by inhibiting the hypoxia associated transcription factors and increasing the levels of antioxidant defense enzymes [J]. *ACS Chem Neurosci*, 2013, **4**(2): 285-294.

Cite this article as: ZHANG Yin-Qiu, WU Jian-Bing, YIN Wei, ZHANG Yi-Hua, HUANG Zhang-Jian. Design, synthesis, and biological evaluation of ligustrazine/resveratrol hybrids as potential anti-ischemic stroke agents [J]. *Chin J Nat Med*, 2020, **18**(8): 633-640.